

# Contrastive Learning-Based Agent Modeling for Deep Reinforcement Learning

Wenhao Ma<sup>1</sup>, Yu-Cheng Chang<sup>1</sup>, Jie Yang<sup>1</sup>, Yu-Kai Wang<sup>1</sup>, Chin-Teng Lin<sup>\*,1</sup>

<sup>1</sup>GrapheneX-UTS Human-centric Artificial Intelligence Centre (HAI),  
University of Technology Sydney,  
Ultimo NSW 2007, Australia

\*Corresponding Author. Email: chin-teng.lin@uts.edu.au

## Abstract

Multi-agent systems often require agents to collaborate with or compete against other agents with diverse goals, behaviors, or strategies. Agent modeling is essential when designing adaptive policies for intelligent machine agents in multi-agent systems, as this is the means by which the ego agent understands other agents' behavior and extracts their meaningful policy representations. These representations can be used to enhance the ego agent's adaptive policy which is trained by reinforcement learning. However, existing agent modeling approaches typically assume the availability of local observations from other agents (modeled agents) during training or a long observation trajectory for policy adaption. To remove these constrictive assumptions and improve agent modeling performance, we devised a Contrastive Learning-based Agent Modeling (CLAM) method that relies only on the local observations from the ego agent during training and execution. With these observations, CLAM is capable of generating consistent high-quality policy representations in real-time right from the beginning of each episode. We evaluated the efficacy of our approach in both cooperative and competitive multi-agent environments. Our experiments demonstrate that our approach achieves state-of-the-art on both cooperative and competitive tasks, highlighting the potential of contrastive learning-based agent modeling for enhancing reinforcement learning.

## Introduction

Conventional multi-agent reinforcement learning methods have limitations in effectively training adaptive policies that enable intelligent agents to efficiently collaborate or compete with partner or adversarial agents employing diverse policies. Researchers have long sought to develop methods that encourage machine agents to efficiently collaborate with agents that have diverse behavioral characteristics, including collaborations human agents (O'Neill et al. 2022). Many multi-agent reinforcement learning methods typically employ Centralized Training with Decentralized Execution (CTDE) architecture (Lowe et al. 2017; Sunehag et al. 2017; Foerster et al. 2016) to construct such collaboration policies. However, although this architecture can yield effective cooperation or competition policies, it is limited by the requirement for consistency among the policies of the agents throughout the training and execution phases. Deviating from this consistency may lead to a breakdown in the

established tacit understanding among agents. Hence, it is evident that conventional multi-agent reinforcement learning frameworks do not necessarily lend themselves well to effectively training adaptive policies that enable intelligent agents to efficiently collaborate or compete with partner or adversarial agents employing diverse policies.

To address this issue, scholars in the field of multi-agent systems have shifted their focus towards the technique of agent modeling (Shoham, Powers, and Grenager 2007; Albrecht and Stone 2018). A highly significant capability of intelligent agents is their capacity to infer the intentions and policies of different agents. For this reason, agent modeling, as a kind of policy representation technique, has become an indispensable and vital component of multi-agent systems.

The extant approaches involve using observation signals from both the ego agent and the modeled agents to generate distinctive policy representations through deep neural network models. These representations, which are commonly referred to as "context information", are then combined with ego agent's real-time observation signals to train adaptive policies for cooperating or competing with other agents via reinforcement learning(Sutton and Barto 2018). Most agent modeling methods either assume that modeled agents' local observation will be available during the training phase, or they rely on a long historical observation trajectories from the ego agent to generate informative policy representation during execution. However, these assumptions or conditions are overly stringent and quite idealized. In the real-world, it can be challenging to gather precise observational information from the modeled agent's perspective-especially when the scenario involves human-autonomy collaborative scenarios and the modeled agent is a human. Futher, waiting for a sufficiently long observation trajectory before commencing policy representation is impractical.

To address these challenges, we devised a novel approach to agent modeling. The basic idea is to treat agent modeling as a representation learning task while leveraging the recent advancements in self-supervised contrastive learning. The key contributions of our method are as follows:

1. We propose a Contrastive Learning-based Agent Modeling (CLAM) model that consists of a Transformer encoder and an attention pooling module. The model generates policy representations of the modeled agent in real time, and only requires the local observations of the ego agents.

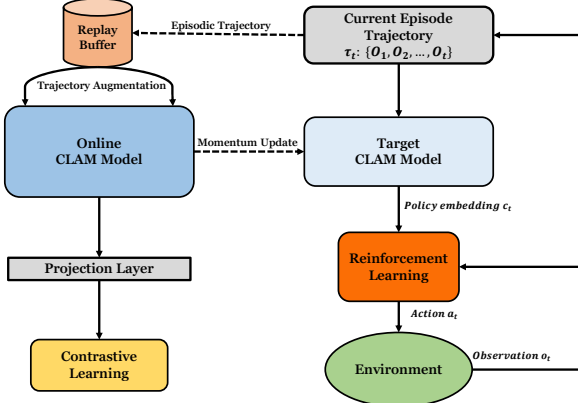


Figure 1: Diagram of our proposed agent modeling model and adaptive policy training architecture. The left part is for CLAM training. The right part is for adaptive policy training.

2. The proposed CLAM is the first model integrating an attention mechanism into the agent modeling field. The attention mechanism allows the CLAM to allocate weights to different parts of local observation based on their importance, thereby enhancing its ability to capture relevant information.

3. The model is trained using self-supervised contrastive learning with accompanying asymmetric sample augmentation method that creates positive sample pairs. The results of comparative experiments demonstrate that our method produces better policy representations than those produced through symmetric sample augmentation techniques.

4. The unified training architecture concurrently trains the agent modeling and reinforcement learning model resulting in a more concise, efficient, and easily deployable framework.

## Related Work

### Agent Modeling

Agent modeling (or opponent modeling) plays a crucial role in the design of adaptive policies for intelligent machine agents within multi-agent systems, as it enables the controlled agent (ego agent) to acquire a deeper comprehension and prediction of the policies of other agents (modeled agents) present in the system. This capacity can be utilized to augment the decision-making process and empower the ego agent to adapt its behavior in accordance with the policies of the modeled agents. (He et al. 2016) proposed a neural network-based model to jointly learn the adaptive policy and agent modeling model. The Theory of mind Network (Tom-Net) (Rabinowitz et al. 2018), used two networks called character net and mental net to infer the goals of modeled agent efficiently. (Grover et al. 2018) proposed an encoder-decoder architecture, which embeds the input observation trajectory into feature vectors in a point-wise manner and uses the average pooling method to generate the representation of the trajectory. (Papoudakis, Christianos, and Albrecht

2021) also based on an encoder-decoder architecture. But they use a recurrent encoder which can better leverage historical observation information to aid the ego agent. These mentioned agent modeling approaches either assume the availability of local observations from other agents (modeled agents) during training or a long observation trajectory for policy adaption. The key distinction between our approach and these studies lies in the fact that we only rely on observations from the ego agent and adapt the ego agent's policy within a few steps.

### Contrastive Learning

In recent years, contrastive learning has emerged as a prominent paradigm in the realm of machine learning and representation learning. The underlying principle of contrastive learning revolves around learning representations by maximizing the similarity between positive pairs and minimizing the similarity between negative pairs (Oord, Li, and Vinyals 2018). This concept has gained widespread interest and has been extensively explored across a spectrum of domains, encompassing computer vision and natural language processing (Jaiswal et al. 2020). Seminal works like SimCLR (Chen et al. 2020) have paved the way by introducing the concept of large-batch training coupled with negative samples to augment the quality of learned representations. Building upon this foundation, MoCo (He et al. 2020) incorporated a momentum moving-averaged encoder to facilitate better feature extraction. Additionally, approaches like SwAV (Caron et al. 2020) have ventured into novel augmentation strategies to enhance contrastive learning.

### Attention Mechanism

The attention mechanism (Bahdanau, Cho, and Bengio 2014) is widely employed in the field of machine learning because of its ability to dynamically adjust the focus on different parts of input data. This allows models to allocate weights to different parts of input data based on their importance, thereby enhancing their ability to capture relevant information. The basic idea of the attention mechanism is to calculate a weighted sum of values based on the relationship between the query and keys, which can be described as follows:

$$\text{Attention}(Q, K, V) = \text{Softmax}\left(\frac{QK^T}{\sqrt{d_k}}\right)V \quad (1)$$

where  $Q$ ,  $K$ , and  $V$  are matrices that represent query, key, and value, respectively.

The Transformer (Vaswani et al. 2017) introduced the multi-head attention mechanism for the first time. This novel attention mechanism enables models to simultaneously learn to focus on different features within multiple subspaces, significantly improving the model's representation capacity. Due to its outstanding performance, the Transformer has found widespread applications in the field of natural language processing (NLP) and computer vision.(Devlin et al. 2018; Radford et al. 2018; Dosovitskiy et al. 2020) Given  $d$ -dimensional query  $Q$ , key  $K$ , value  $V$ , and  $n$  attention heads, each with its own weight matrices  $W_n^Q \in \mathbb{R}^{d \times d_k}$ ,

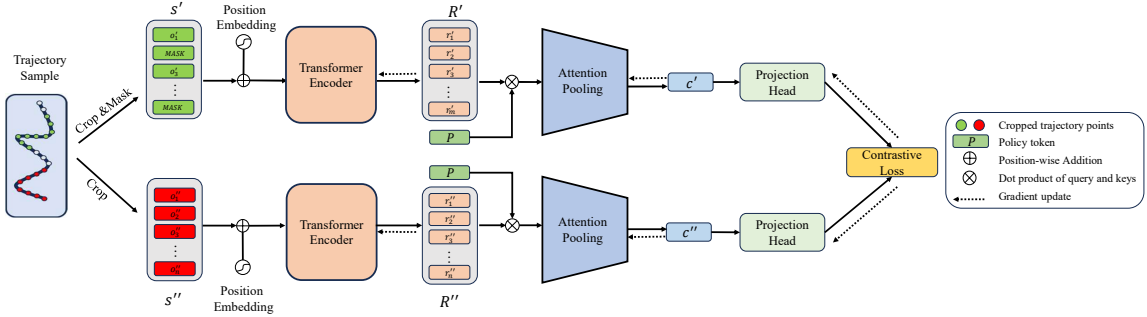


Figure 2: Diagram of CLAM model training process.

$W_n^K \in \mathbb{R}^{d \times d_k}$ ,  $W_n^V \in \mathbb{R}^{d \times d_v}$ ,  $d_k = d_v = d/n$ . The computation of multi-head attention can be expressed as follows:

For the  $n$ th head  $h_n$ :

$$h_n = \text{Attention}(QW_n^Q, KW_n^K, VW_n^V)$$

Then, the outputs of each head are concatenated and linearly transformed to obtain the final output of multi-head attention:

$$\text{MultiHead}(Q, K, V) = \text{concat}(h_1, h_2, \dots, h_n)W^O \quad (2)$$

where  $W^O$  is a trainable weight matrix used for linear transformation.

## Method

### Problem Statement

In this chapter, we formally introduce the problem to be addressed. Overall, our goal is to create an intelligent machine agent (ego agent) that, using its local observation to infer the intentions, behavioral preferences, policies, and other characteristics of other agents (modeled agents) within the same environment. Through training, the ego agent will be given the ability to interact efficiently with the modeled agents that execute different policies picked from a diverse policy set.

This entire problem can be modeled as a Partially Observable Markov Game (POMG) (Littman 1994) involving  $N$  agents, defined as the tuple  $(I, S, A, O, T, R, \Omega)$ . Here,  $I = \{1, \dots, n\}$  represents the set of agents.  $S$  represents the set of states,  $A = A_1 \times A_2 \times \dots \times A_N$  is the joint action space and  $O = O_1 \times O_2 \times \dots \times O_N$  is joint observation space.  $T$  represents the transition function, where  $T : S \times A \rightarrow S$  and  $R$  represents the reward function, where  $R : S \times A \rightarrow \mathbb{R}$ ,  $\Omega$  is the observation function, which defines the probability distribution of the next observation given the current observation and action,  $\Omega : S \times A \times O \rightarrow [0, 1]$ .

To ensure clarity and precision, we use "m" and "e" to label the modeled agent and the ego agent, e.g.,  $o^m$  and  $o^e$  represent the local observations of the modeled agent and the ego agent, respectively. It is assumed that a set of predefined fixed policies exists  $\Pi = \{\pi_i^m | i = 1, 2, \dots, n\}$ , which can either be hand-coded or created via reinforcement learning. The policies within this policy set are randomly selected and made available for execution by the modeled agent. A fixed

policy  $\pi_i^m(a_t^m | o_t^m)$  represents a function that maps the modeled agent's current observation  $o_t^m$  to a distribution over its action  $a_t^m$ . Our objective is to train the ego agent's adaptive policy  $\pi_\alpha$ , which is parameterized by  $\alpha$ , to achieve the maximum expected reward through interactions with the policies in the fixed policy set  $\Pi$ :

$$\mathbb{E}_{\pi_i^m \sim u(\Pi)} [\mathbb{E}_{\pi_\alpha, \pi_i^m} [\sum_{t=0}^{T-1} \gamma^t r_t(o_t^e, a_t^e)]] \quad (3)$$

where the inner expectation accounts for the discounted cumulative reward acquired by the ego agent throughout one episode length  $T$  and the outer expectation accounts for the ego agent's average episodic reward over various policies  $\pi_i^m$  of the modeled agent. The policy  $\pi_i^m$  is drawn from a uniform distribution  $u(\Pi)$ .  $r_t(\cdot)$  is the ego agent's reward function and  $\gamma \in (0, 1)$  is the discount factor to balance the trade-off between immediate return and long-term return.

### Contrastive Learning-based Agent Modeling (CLAM)

To address our research problem, an agent modeling model needs to be constructed to generate real time policy representation. As its input, this model takes an observation trajectory of the ego agent from the beginning of an episode 0 up to the current time  $t$ , i.e.,  $\tau_t = \{o_i^e\}_{i=0:t}$ . It then generates and outputs a policy representation vector  $c_t$ . This vector is intended to encapsulate the policy-specific information of the modeled agent, including its objectives, its behavioral characteristics, and policy information. This real-time policy representation vector  $c_t$  will be used in conjunction with the real-time observations  $o_t^e$  of the ego agent to condition the adaptive policies as  $\pi_\alpha(a_t | o_t^e, c_t)$ .

In this work, the agent modeling model CLAM is composed of two components: (1) a Transformer encoder to transform the original observation trajectory  $\tau_t$  into corresponding feature representation sequence  $\{r_i\}_{i=0:t}$ ; (2) an attention pooling module to aggregation the temporal feature sequence  $\{r_i\}_{i=0:t}$  into a policy representation vector  $c_t$ . Next, how the two components are constructed will be described in detail.

**Transformer Encoder:** The observation trajectory of the ego agent can be considered a form of sequential data, which

naturally prompted us to consider using a Transformer encoder  $f_\theta(\cdot)$ , parameterized by  $\theta$ , to capture patterns and relationships within the ego agent's observation trajectories. We leverage the standard Transformer encoder (Vaswani et al. 2017) which consists of multiple multi-head self-attention and multilayer perceptron (MLP) blocks. Firstly, we encode the ego agent's observation trajectory  $\tau_t$  with position embeddings to retain temporal information. The embedded trajectory is then fed into the Transformer encoder to create the feature embedding sequence  $\{r_i\}_{i=0:t}$  as  $\{r_i\}_{i=0:t} = f_\theta(\tau_t)$ .

**Attention Pooling Module:** After the Transformer encoder generates the feature embedding vector  $\{r_i\}_{i=0:t}$  for each episode step within the observation trajectory, the next step is to aggregate the feature embedding sequence into a single policy representation vector for the current interaction episode. Conventional methods usually employ average pooling (Rabinowitz et al. 2018; Grover et al. 2018) for this feature aggregation step. However, since each vector in the trajectory might have a different contribution to the final policy representation vector, we believe that using an attention mechanism might better capture complex temporal relationships and patterns within the trajectory. Thus, our model appends an attention pooling module  $pool_\phi(\cdot)$  parameterized by  $\phi$  after the Transformer encoder. We create a special trainable policy token  $P \in \mathbb{R}^{1 \times d}$  as the query in the attention mechanism to aggregate the feature embedding sequence  $R_t = \{r_i\}_{i=0:t}$ , following equation (2), attention pooling function  $pool_\phi(\cdot)$  with policy token  $P$  is defined as

$$pool_\phi(R_t) = rFF(MultiHead(P, R_t, R_t)) \quad (4)$$

where  $rFF$  is row-wise feedforward layers.

This policy token  $P$  helps to aggregate the entire input feature vector sequence  $R_t$  into a single policy representation vector  $c_t$ . Our experiments also verify that attention-based pooling helps the agent to get higher rewards compared to average pooling. A detailed analysis can be found in the ablation study.

**Contrastive Learning Training:** We optimize the parameters of the transformer encoder  $\theta$  and attention-based pooling module  $\phi$  through self-supervised contrastive learning. The overall training process is depicted in Fig. 2. Firstly, We select a batch of size  $N$  observation trajectories  $\{\tau_i\}_{i=1:N}$  from the replay buffer. Then, we randomly crop two trajectory windows from each sampled trajectory and form two sample sets  $S = \{s_i\}_{i=1:N}$  and  $S' = \{s'_i\}_{i=1:N}$ . The two cropped samples  $s_i$  and  $s'_i$  extracted from the same original trajectory  $\tau_i$  can be considered positive sample pairs, while trajectory samples cropped from different original trajectory samples serve as negative sample pairs. Subsequently, we conduct secondary sample augmentation on one sample set  $S$ . This involves randomly masking a certain ratio of observation steps in the trajectory sample, resulting in a new sample set  $S''$ , while the other sample set  $S'$  remains unaltered. The masked observation steps are replaced with 0. The sample set  $S''$  subjected to mask-based augmentation is termed "strong augmentation," while the unaltered one  $S'$  is referred to as "weak augmentation". This asymmetric sample augmentation approach has been experimentally shown

to enhance the performance of contrastive learning models (Wang et al. 2022). We believe the underlying rationale for our asymmetric sample augmentation approach is to compel the model to extract more representative policy features from sparser and less informative observation trajectories. This approach enhances the model's ability to capture subtle patterns, making it more adept at handling real-time policy representation tasks.

We utilize the InfoNCE loss proposed in (Oord, Li, and Vinyals 2018) as the loss function for contrastive learning:

$$\mathcal{L}_C(\theta, \phi) = -\frac{1}{N} \sum_{i=1}^N \log \frac{\exp(\mathbf{c}'_i \cdot \mathbf{c}''_i / \delta)}{\sum_{k=1}^N \exp(\mathbf{c}'_i \cdot \mathbf{c}''_k / \delta)} \quad (5)$$

where  $N$  is the batch size,  $\delta$  is a temperature parameter,  $\mathbf{c}'_i$  and  $\mathbf{c}''_i$  is a positive pair of policy representations and  $\mathbf{c}''_k$  is any other samples generated by the agent modeling model. Note that a projection head is also used, which is the same as in (Chen et al. 2020).

## Reinforcement Learning Training

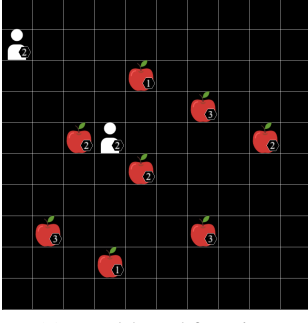
Reinforcement learning is employed to train adaptive policies. The real-time output policy representation vector  $c_t$  from the agent modeling mode is combined with the agent's observation state  $o_t$ , to condition the optimal policy, i.e.,  $\pi_\alpha(a_t|o_t, c_t)$ . As a result, the trained agent policy can generate optimal action outputs specialized for the representation information  $c_t$ . In this paper, we select PPO (Schulman et al. 2017) as the backbone algorithm for reinforcement learning training. However, it's important to note that other reinforcement learning algorithms can also be equally applicable. The specific objective function is defined as follows:

$$\begin{aligned} L_{PPO}(\alpha) = \mathbb{E} \left[ \min \left( \frac{\pi(\alpha, a_t|o_t, c_t)}{\pi_{\text{old}}(a_t|o_t, c_t)} \cdot A_t, \right. \right. \\ \left. \left. \text{clip} \left( \frac{\pi(\alpha, a_t|o_t, c_t)}{\pi_{\text{old}}(a_t|o_t, c_t)}, 1 - \epsilon, 1 + \epsilon \right) \cdot A_t \right) \right] \\ - c \cdot \mathbb{E} [H(\pi(\alpha|o_t, c_t))] \end{aligned} \quad (6)$$

where  $A_t$  is the advantage function, representing the advantage of taking action  $a_t$  with observation  $o_t$ ,  $H(\cdot)$  is the entropy function,  $c$  is the coefficient of entropy regularization and  $\text{clip}(\cdot)$  is a clipping function used to restrict the magnitude of policy updates.

## Experiment Environment

We selected two representative multi-agent environments to evaluate our method: a cooperative environment, level-based foraging (Christianos, Schäfer, and Albrecht 2020; Papoudakis et al. 2020) and a competitive environment, predator-prey (Mordatch and Abbeel 2018). We created a fixed policy set of ten policies for each environment. At the beginning of each episode, a policy is randomly selected from the policy set with equal probability and assigned to the modeled agent.



(a) Level-based foraging.



(b) Predator prey.

Figure 3: The two multi-agent environments for evaluation.

**Level-based Foraging:** This is a grid environment consisting of two agents and a number of apples, as shown in Fig. 3(a). Each agent and apple has its own level value, and the agent has six action options: up, down, left, right, stay still, and pick apple. Agents can successfully pick up an apple when one or both agents are located in one of the four grid cells adjacent to the targeted apple and the sum of the agents' levels is not less than the apple's level. When an apple is picked up, each agent receives a reward based on their contribution to completing the task. The total reward value for each episode is normalized to 1. An episode ends when all apples are picked up or after 50 time steps. In this environment, one of the agents serves as the modeled agent while the other agent is the ego agent and is trained via reinforcement learning. Since our aim is to assess the model's performance in a cooperative environment, we compute the total reward obtained by both agents as a team in each episode. A higher value indicates more efficient cooperation among the agent team.

**Predator-prey:** This competitive multi-agent environment consists of three predators, one prey, and two circular obstacles, as illustrated in Fig. 3(b). Each agent has five action options: up, down, left, right, and stay still. The three predators are assigned fixed policy combinations, while the prey is the ego agent under training. The reward setting in the environment is such that when a predator collides with the prey, the prey receives -10 and the predator receives +10. In the event of a predator-predator collision, each predator receives -3 and the prey receives +3. This reward scheme encourages the prey to learn adversarial policy by evading the predator team's pursuit while inducing more chaos and collisions among them. This environment is highly suitable for evaluating the effectiveness and performance of agent modeling methods. By employing agent modeling methods to acquire informative policy representations, the ego agent can learn targeted adversarial policy based on different opponent policies to obtain greater rewards. Each episode in this environment lasts for 50 time steps.

## Baseline Methods

We chose two widely recognized and representative methods in the field of agent modeling as baselines for our compar-

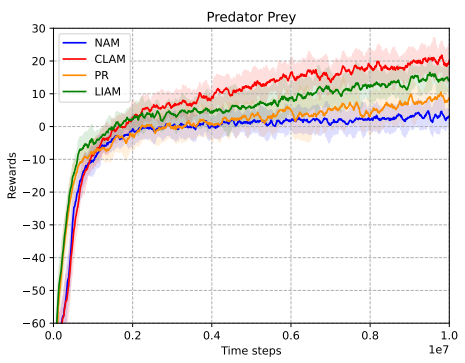
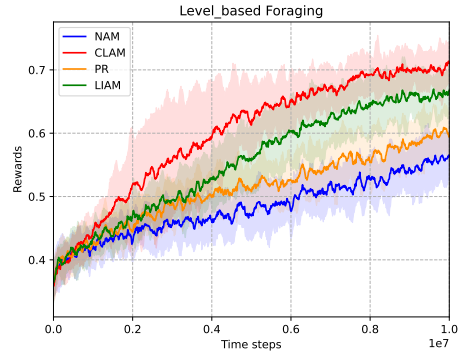


Figure 4: Episodic evaluation returns and 95% confidence interval of the four evaluated methods in two scenarios.

ative experiments. Additionally, we included a naïve PPO method that does not involve agent modeling as another baseline.

**No Agent Modeling (NAM):** Since this approach does not employ any agent modeling techniques, we expect this to be the worst of the methods. NAM merely serves as a benchmark to evaluate whether agent modeling methods do anything to enhance the ego agent's policy performance and, if so, to quantify the degree of that improvement.

**Policy Representation Learning in Multi-Agent System (PR):** This baseline is based on the method proposed by (Grover et al. 2018). The method is built on an encoder-decoder architecture, where the encoder embeds the input observation trajectory into feature vectors in a point-wise manner, yielding vectors for each time step within the trajectory. The feature vectors are aggregated using the average pooling method to obtain the trajectory's representation. This approach generally requires modeling an ego agent's complete observation trajectory from a previous episode to generate the modeled agent's policy representation.

**Local Information Agent Modeling (LIAM):** This baseline was introduced by (Papoudakis, Christianos, and Albrecht 2021). Like PR, it employs an encoder-decoder architecture. But unlike PR, the encoder is a recurrent encoder. The encoder takes in the history of the ego agent's observa-

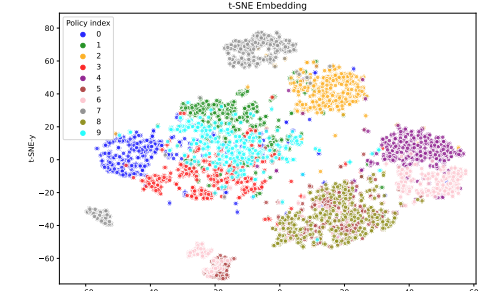
tions and actions up to the current time step and outputs the modeled agent’s policy representation  $c_t$  in real time during the current episode. This method requires obtaining the modeled agent’s observations and actions for the reconstruction task during the training phase but only needs the ego agent’s observations and actions during the execution.

## Policy Evaluation

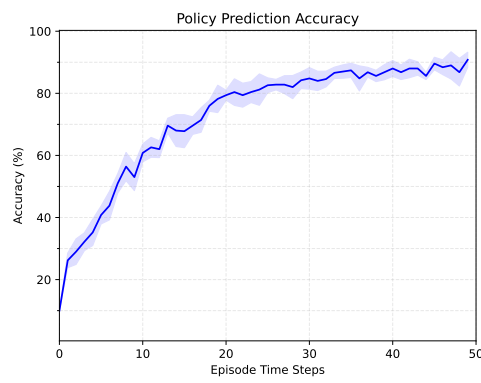
Fig. 4 shows the average reward curves for the three baselines and CLAM in two multi-agent environments. We trained each method for 10 million time steps, conducting evaluations every 10,000 time steps. We evaluated each method using five different random seeds. The solid lines represent the average reward values over five separate runs, while the shaded regions indicate the 95% confidence interval. From the figure, it is evident that the NAM baseline performs the worst in both environments, in line with our expectations. Naïve reinforcement learning algorithms without agent modeling modules cannot acquire any auxiliary information to distinguish between the policies of its opponents or teammates. The PR method performed slightly better than NAM in both environments but fell short compared to the other two methods. We attribute this outcome to the point-wise encoding approach of PR, which does not seem to effectively capture temporal relationships between trajectory steps. This limitation results in so few informative policy representation vectors that the model cannot accurately model the agents’ strategy features. Hence, the representation provide little assistance in the ego agent’s adaptive policy training. Additionally, using the average pooling method to aggregate feature vectors might not be the optimal approach. LIAM, which employs a recurrent encoder, receives the second-highest rewards (on average) in both scenarios. This method capitalizes on the temporal information within trajectories for effective representation learning, resulting in policy representations with richer information than PR. As can be seen, the performance improvement is substantial compared to the other two baselines. CLAM achieved the highest rewards in both environments. We reason this is due to the attention mechanism, which captures long-range temporal patterns within the trajectory sequences. Moreover, CLAM employs the mask method in the sample augmentation step of contrastive learning. This enhances the model’s capability to identify the most distinctive feature information within the trajectories of different policies, resulting in superior performance.

## Model Evaluation

Continuing our analysis, we delve into why the CLAM method achieves such remarkable performance. Utilizing the t-SNE method (Van der Maaten and Hinton 2008), we projected the policy representation embeddings into a two-dimensional space, as shown in Fig. 5(a). These were the policy embeddings output by CLAM’s encoder at the 25th time step of each episode in the Predator-prey environment. Each color represents a different fixed policy combination for the predator team, and each point represents an episode. From the figure, it is apparent that points of the same color are strongly clustered. This is a good indication that the



(a)



(b)

Figure 5: (a) t-SNE projection of the embeddings in the predator-prey environment, where different colors represent different fixed policies and different points represent different episodes. (b) Policy prediction accuracy.

CLAM model can identify and differentiate the behavioral characteristics of different predator team policies.

However, we did notice an overlap between Policy 5 and Policy 8. Further examination reveals that these two policy combinations inherently share similar features. As a result, the self-supervised contrastive learning scheme struggled to tell them apart. Nevertheless, this underscores that CLAM can indeed represent policies based on their behavioral similarities, effectively aiding the training of adaptive cooperative or adversarial policies through reinforcement learning.

Subsequently, we verified the rapid generation of informative real-time policy representations by freezing the policy encoder’s parameters and attaching a prediction head composed of MLPs. We input the complete episodic observation trajectories’ representation embeddings into the prediction head. The prediction head uses the policy class labels as supervision signals to predict the corresponding class for each policy representation embedding.

After training, we tested the predictive accuracy of policy representations for observation trajectories of lengths from 0 to 49, the idea being to validate the model’s representation capabilities. The results appear in Fig. 5(b). The solid line represents the average accuracy over five tests, while

the shaded region denotes the 95% confidence interval.

From the figure, we can see that, at time step 0, the representations are random due to the lack of sufficient temporal information available, and so the result is an average accuracy of 10% for predicting the 10 policies. However, as the time steps progress, the accuracy rapidly increases, reaching around 60% at step 10, close to 80% at step 20, and surpassing 90% accuracy for full trajectory representations at the final step of 49. This demonstrates that the CLAM method can generate informative representations early in each episode and ensure high consistency in the representation space across trajectory lengths.

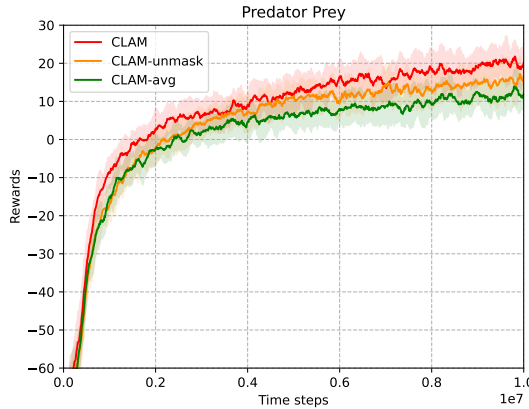


Figure 6: Average rewards comparison of CLAM against two ablated versions of CLAM in predator-prey environment.

### Ablation Study

This section presents the results of an ablation study we conducted to better understand the impact of different designs in our CLAM model. Our two assessment metrics were: i) the average rewards obtained by the agents in a multi-agent environment, and ii) the Intra-Inter Clustering Ratio (IICR) of the policy embeddings. IICR essentially assesses the clustering properties of feature vectors in an embedding space. It is a valuable metric for evaluating the feature learning capability of self-supervised methods and the discriminative power of learned features in representing diverse sample classes. An IIRC value of less than 1 indicates the effectiveness of the feature representation method in aggregating similar samples and separating dissimilar samples. The smaller the value, the more pronounced the clustering effect and the better model’s representation performance. We evaluated two ablated versions of CLAM: CLAM-avg which replaced the attention pooling module with the average pooling method and CLAM-unmask which did not use the mask-based sample augmentation method.

Fig. 6 illustrates the average reward curves for CLAM and CLAM-avg. It is evident from the figure that CLAM yields higher average rewards. Table 1 presents the IICR results. We scored the policy embeddings at time steps (10, 20, 30, 40, 50). From a comparison of the score, it is clear that the values for CLAM are consistently lower than those of CLAM-avg, indicating its superior representation

Method \ Time step	10	20	30	40	50
CLAM	<b>0.89</b>	<b>0.78</b>	<b>0.75</b>	<b>0.74</b>	<b>0.74</b>
CLAM-avg	0.94	0.88	0.85	0.83	0.82
CLAM-unmask	0.89	0.83	0.81	0.80	0.79

Table 1: Intra-Inter Clustering Ratios (IICR) of policy representation embeddings in predator-prey environment.

performance. We attribute this to the attention pooling module’s ability to better focus on crucial temporal features in the ego agent’s observation trajectories resulting in a more distinct aggregation of feature vectors and ultimately yielding more informative policy representations.

Our next experiment was to test the mask-based sample augmentation technique. Comparing CLAM and CLAM-unmask in Fig. 6, CLAM amassed higher rewards. The IICR values also suggest that CLAM outperforms CLAM-unmask in terms of policy representation clustering. This indicates that incorporating a mask-based asymmetric sample augmentation method enhances the model’s policy representation ability. Based on our empirical insights, we conjecture that the model is forced to rely on the remaining unmasked portions to capture the most essential and discriminative features. This would lead to more focused learning of the important temporal patterns and relationships within the observation trajectory. Again, the result is more robust and informative embeddings that capture the essential characteristics of the modeled agents’ policies.

### Conclusion

This paper presented a novel agent modeling model that leverages a Transformer encoder and an attention pooling module. The model effectively captures real time policy representations of the modeled agents, utilizing only the observation signals from the ego agent. Importantly, our work pioneers the integration of the attention mechanism into the field of agent modeling. This innovative attention mechanism empowers the proposed model to efficiently learn how to capture useful information from the ego agent’s local observation, thereby substantially augmenting the model’s capacity for representation. Through contrastive learning, and combined with an innovative asymmetric sample augmentation technique for creating positive sample pairs, we successfully trained a model to model agent policies in a self-supervised manner. Our experimental results demonstrate that CLAM significantly increases the episodic rewards obtained by the ego agent compared to baseline methods. More importantly, in contrast to the baseline methods, our approach stands out by eliminating the necessity to acquire observations from the perspective of the modeled agent or to rely on long-range trajectories. It exclusively relies on the observations of the ego agent as the model’s input. In the future, we will use the CLAM model in human-machine collaboration environments. The proposed approach has the potential to enhance the versatility of multi-agent reinforcement learning methods, making them applicable to scenarios involving human-machine collaboration to achieve a common goal, such as in manufacturing or logistics.

## References

Albrecht, S. V.; and Stone, P. 2018. Autonomous agents modelling other agents: A comprehensive survey and open problems. *Artificial Intelligence*, 258: 66–95.

Bahdanau, D.; Cho, K.; and Bengio, Y. 2014. Neural machine translation by jointly learning to align and translate. *arXiv preprint arXiv:1409.0473*.

Caron, M.; Misra, I.; Mairal, J.; Goyal, P.; Bojanowski, P.; and Joulin, A. 2020. Unsupervised learning of visual features by contrasting cluster assignments. *Advances in neural information processing systems*, 33: 9912–9924.

Chen, T.; Kornblith, S.; Norouzi, M.; and Hinton, G. 2020. A simple framework for contrastive learning of visual representations. In *International conference on machine learning*, 1597–1607. PMLR.

Christianos, F.; Schäfer, L.; and Albrecht, S. 2020. Shared experience actor-critic for multi-agent reinforcement learning. *Advances in neural information processing systems*, 33: 10707–10717.

Devlin, J.; Chang, M.-W.; Lee, K.; and Toutanova, K. 2018. Bert: Pre-training of deep bidirectional transformers for language understanding. *arXiv preprint arXiv:1810.04805*.

Dosovitskiy, A.; Beyer, L.; Kolesnikov, A.; Weissenborn, D.; Zhai, X.; Unterthiner, T.; Dehghani, M.; Minderer, M.; Heigold, G.; Gelly, S.; et al. 2020. An image is worth 16x16 words: Transformers for image recognition at scale. *arXiv preprint arXiv:2010.11929*.

Foerster, J.; Assael, I. A.; De Freitas, N.; and Whiteson, S. 2016. Learning to communicate with deep multi-agent reinforcement learning. *Advances in neural information processing systems*, 29.

Grover, A.; Al-Shedivat, M.; Gupta, J.; Burda, Y.; and Edwards, H. 2018. Learning policy representations in multiagent systems. In *International conference on machine learning*, 1802–1811. PMLR.

He, H.; Boyd-Graber, J.; Kwok, K.; and Daumé III, H. 2016. Opponent modeling in deep reinforcement learning. In *International conference on machine learning*, 1804–1813. PMLR.

He, K.; Fan, H.; Wu, Y.; Xie, S.; and Girshick, R. 2020. Momentum contrast for unsupervised visual representation learning. In *Proceedings of the IEEE/CVF conference on computer vision and pattern recognition*, 9729–9738.

Jaiswal, A.; Babu, A. R.; Zadeh, M. Z.; Banerjee, D.; and Makedon, F. 2020. A survey on contrastive self-supervised learning. *Technologies*, 9(1): 2.

Littman, M. L. 1994. Markov games as a framework for multi-agent reinforcement learning. In *Machine learning proceedings 1994*, 157–163. Elsevier.

Lowe, R.; Wu, Y. I.; Tamar, A.; Harb, J.; Pieter Abbeel, O.; and Mordatch, I. 2017. Multi-agent actor-critic for mixed cooperative-competitive environments. *Advances in neural information processing systems*, 30.

Mordatch, I.; and Abbeel, P. 2018. Emergence of grounded compositional language in multi-agent populations. In *Proceedings of the AAAI conference on artificial intelligence*, volume 32.

Oord, A. v. d.; Li, Y.; and Vinyals, O. 2018. Representation learning with contrastive predictive coding. *arXiv preprint arXiv:1807.03748*.

O’Neill, T.; McNeese, N.; Barron, A.; and Schelble, B. 2022. Human–autonomy teaming: A review and analysis of the empirical literature. *Human factors*, 64(5): 904–938.

Papoudakis, G.; Christianos, F.; and Albrecht, S. 2021. Agent modelling under partial observability for deep reinforcement learning. *Advances in Neural Information Processing Systems*, 34: 19210–19222.

Papoudakis, G.; Christianos, F.; Schäfer, L.; and Albrecht, S. V. 2020. Benchmarking multi-agent deep reinforcement learning algorithms in cooperative tasks. *arXiv preprint arXiv:2006.07869*.

Rabinowitz, N.; Perbet, F.; Song, F.; Zhang, C.; Eslami, S. A.; and Botvinick, M. 2018. Machine theory of mind. In *International conference on machine learning*, 4218–4227. PMLR.

Radford, A.; Narasimhan, K.; Salimans, T.; Sutskever, I.; et al. 2018. Improving language understanding by generative pre-training.

Schulman, J.; Wolski, F.; Dhariwal, P.; Radford, A.; and Klimov, O. 2017. Proximal policy optimization algorithms. *arXiv preprint arXiv:1707.06347*.

Shoham, Y.; Powers, R.; and Grenager, T. 2007. If multi-agent learning is the answer, what is the question? *Artificial intelligence*, 171(7): 365–377.

Sunehag, P.; Lever, G.; Gruslys, A.; Czarnecki, W. M.; Zambaldi, V.; Jaderberg, M.; Lanctot, M.; Sonnerat, N.; Leibo, J. Z.; Tuyls, K.; et al. 2017. Value-decomposition networks for cooperative multi-agent learning. *arXiv preprint arXiv:1706.05296*.

Sutton, R. S.; and Barto, A. G. 2018. *Reinforcement learning: An introduction*. MIT press.

Van der Maaten, L.; and Hinton, G. 2008. Visualizing data using t-SNE. *Journal of machine learning research*, 9(11).

Vaswani, A.; Shazeer, N.; Parmar, N.; Uszkoreit, J.; Jones, L.; Gomez, A. N.; Kaiser, Ł.; and Polosukhin, I. 2017. Attention is all you need. *Advances in neural information processing systems*, 30.

Wang, X.; Fan, H.; Tian, Y.; Kihara, D.; and Chen, X. 2022. On the importance of asymmetry for siamese representation learning. In *Proceedings of the IEEE/CVF Conference on Computer Vision and Pattern Recognition*, 16570–16579.